

Mini-Project (ML for Time Series) - MVA 2025/2026

Adonis Jamal adonis.jamal@student-cs.fr
Fotios Kapotos fotiskapotos@gmail.com

December 14, 2025

1 Introduction and contributions

In modern sports analytics, identifying team formations is essential for interpreting tactics. However, tracking data in fluid sports like soccer is noisy; players frequently swap positions temporarily, making it difficult to distinguish permanent tactical shifts from transient adjustments. To address this, we examine SoccerCPD [2], a change-point detection framework designed to identify distinct tactical phases. The method operates in two stages: first, FormCPD detects formation changes using role-adjacency matrices derived from Delaunay triangulations. Second, RoleCPD identifies role swaps within those formations using permutation sequences.

Contributions and Work Repartition In alignment with the course requirements, this report details our reproduction and extension of the SoccerCPD framework:

Work Repartition: The workload followed the pipeline's structure. One student focused on the **FormCPD** stage, implementing the Delaunay-based adjacency generation and formation change detection. The other concentrated on **RoleCPD**, handling the generation of synthetic role data, permutation analysis, and the recursive segmentation algorithm.

Source Code & Implementation: We adapted the SoccerCPD code to be used as a python package. We also reproduced the core analysis by implementing it in Python, integrating an R-based backend for the Generalized Edge-Count test (g-segmentation) to improve detection accuracy. We also implemented a Python-based fallback for change-point detection to ensure robustness when the R-bridge encounters errors.

Experiments: We verified the method on synthetic datasets, successfully detecting ground-truth change points. We also performed a sensitivity analysis using the provided source code. For real-world applications, we analyzed a Barcelona match, specifically detecting tactical phases and visualizing role allocations.

Novel Analysis: Beyond reproduction, we extended the analysis by introducing a "Player Stationarity" metric. This measures the spatial standard deviation of players to quantify how "fixed" or "fluid" a role is. Furthermore, we refined the formation analysis by separating frames based on Possession Context (Attack vs. Defense), allowing for a more granular understanding of team shape during different game states.

2 Methodology

2.1 Formation Change-Point Detection (FormCPD)

FormCPD converts raw player trajectories $X(t) \in \mathbb{R}^{N \times 2}$ into a temporal sequence of role-based formation graphs $\{A(t)\}_{t \in T}$. Discrete g-segmentation is then applied to detect change-points $T_1 < \dots < T_m$ such that formations are stationary within each segment. Finally, formation segments are aligned and clustered to extract canonical formation types.

2.1.1 Role Assignment

Players are assigned to latent spatial roles following [1], modeling stable positional zones rather than player identities. Each role k is represented by a Gaussian component (μ_k, Σ_k) with the constraint that each role is occupied by exactly one player per frame.

Parameters are estimated via a constrained EM algorithm: the E-step solves a one-to-one assignment using Hungarian matching on negative log-likelihoods, while the M-step updates role parameters from all assigned positions across time.

2.1.2 Change-Point Detection on Graphs via Delaunay Triangulation

Given role locations $V(t) = \{v_1(t), \dots, v_N(t)\}$, each frame is encoded as a role-adjacency graph using Delaunay triangulation. Two roles are connected if they share an edge in the triangulation, producing a binary adjacency matrix $A(t) \in \{0, 1\}^{N \times N}$. Formation changes are detected on the sequence $\{A(t)\}$ using discrete g-segmentation [3]. Dissimilarity between frames is measured by the Manhattan distance. Frames with excessive role switching (rate > 0.7) are discarded. Candidate change-points are retained if they satisfy constraints on statistical significance ($p < 0.01$), minimum segment duration (5 minutes), and inter-segment dissimilarity. A recursive procedure recovers multiple change-points, partitioning the match into formation intervals.

2.1.3 Formation Clustering

Each segment T_i is summarized by a formation graph $F(T_i) = (V(T_i), A(T_i))$, obtained by averaging role positions and adjacency matrices over stable frames. Since role labels are arbitrary across segments, formations are aligned using Hungarian matching on Euclidean distances between $V(T_i)$ and $V(T_j)$, yielding a permutation matrix Q .

Formation similarity is defined as

$$d(F_i, F_j) = \|QA(T_i)Q^\top - A(T_j)\|_{1,1},$$

capturing differences in topological structure. Agglomerative hierarchical clustering on these distances produces a small set of canonical formation types.

2.2 Role CPD

The goal of RoleCPD [2] is to detect long-term tactical changes in player roles (e.g., a winger swapping sides with another winger permanently) while ignoring temporary switches (e.g., overlapping runs or covering defensive duties). This process operates within a single Formation Period (T_i) identified in the previous step. Figure 4 in Appendix B illustrates the ground truth of such role assignments with simulated tactical switches.

2.2.1 Formal Representation

We define the inputs and mathematical framework based on the SoccerCPD protocol:

Input: A sequence of "Temporary Role Permutations" $\{\pi_t\}_{t=1}^{|T_t|}$.

Role Permutation (π_t): At every frame t , the Role Representation step assigns a role X_p to every player p . Since roles are distinct, this assignment is a permutation of the initial canonical role:

$$\beta_t(p) = \pi_t(X_p)$$

Where β_t is the player-to-temporary-role mapping at time t .

2.2.2 The Distance Metric

To detect a change, we must quantify the difference between the team's configuration at time t and time t' . Since the data consists of permutations (non-Euclidean), we cannot use standard Euclidean distance. We use the Hamming Distance normalized by the number of roles ($N = 10$ outfield players):

$$d(\pi_t, \pi_{t'}) = \frac{1}{N} \sum_{p \in P} \mathbb{1}_{\pi_t(X_p) \neq \pi_{t'}(X_p)}$$

This metric represents the "Switch Rate" or the proportion of players whose roles differ between two frames. Figure 5 plots this switch rate over time, showing it fluctuates relative to a dominant permutation.

2.2.3 Change-Point Detection Algorithm

The paper utilizes Discrete g-segmentation, a graph-based change-point detection method effective for repeated observations in non-Euclidean space. The procedure is as follows:

1. **Preprocessing:** Calculate the Switch Rate relative to the dominant permutation. Exclude frames with a switch rate > 0.7 (likely temporary switches during set-pieces or abnormal situations).
2. **Segmentation:** Apply the detection algorithm recursively on the sequence of permutations using the Hamming distance. Figure 6 shows the result of a single segmentation step, while Figure 7 demonstrates the final output after recursive segmentation captures all tactical phases, accurately recovering the ground truth on the synthetic example.
3. **Significance Test:** A change point τ is significant if: the p-value of the scan statistic is < 0.01 , the segmentation duration is sufficient (robustness against noise), and the most frequent permutations (Instructed Roles) in the segments before and after τ must be distinct.

3 Data

Our study utilizes and analyzes two distinct spatiotemporal dataset types: high-frequency GPS tracking data and event-stream data.

High-Frequency Tracking Data: We utilized the provided sample dataset and supplementary public data from SkillCorner (A-League, 10 Hz) and Last Row (20 Hz). All inputs were converted to the Fitgether format (K-League, 10 Hz), represented as a sequence of 2D coordinates $x_{i,t} \in \mathbb{R}^2$.

- **Diagnosis:** The signals are clean (missing values <1%) but exhibit high-frequency jitter consistent with GPS noise. Shapiro-Wilk tests on role clusters indicate deviations from normality due to tactical behaviors (e.g., pressing), yet clusters remain sufficiently separable for EM algorithm convergence.
- **Preprocessing:** We normalized pitch coordinates to a centered metric system to satisfy the model’s Gaussian distribution assumption.

StatsBomb Event Data: To address the scarcity of tracking data, we adapted StatsBomb event-stream data, which records location (x, y) only during on-ball actions.

- **Challenges:** The data exhibits extreme sparsity (<10 points/min vs. ≈ 600 for GPS) and inherent spatial bias toward the ball, challenging the EM algorithm’s density requirements.
- **Adaptation:** We projected coordinates ($[0, 120] \times [0, 80]$) to the centered metric system. To mitigate sparsity, we generated pseudo-trajectories by aggregating events over temporal windows. Finally, we replaced frame-wise Delaunay graphs with aggregate adjacency matrices based on 5-minute average positions to serve as a proxy for the role-adjacency matrix.

4 Results

4.1 Experiments using SoccerCPD

We directly use the SoccerCPD implementation of [2] (with slight practical modifications)

Comparison across CPD backends (single match). We compare several formation CPD backends (`gseg_avg`, `gseg_union`, `kernel_rbf`, `kernel_linear`) on a single reference match, using identical preprocessing and hyperparameters. The objective is not to rank methods, but to assess whether different CPD formulations produce consistent formation change-point timelines.

As shown in Figure 9, all backends detect formation changes at broadly similar temporal locations. Differences mostly correspond to additional or missing change-points rather than large temporal shifts, indicating variations in sensitivity rather than fundamentally different segmentations of the match.

Sensitivity analysis of formation CPD. We analyze the sensitivity of the formation CPD pipeline to its main hyperparameters on the same match, using the `gseg_avg` backend and varying one parameter at a time.

Figure 10 illustrates the effect of the formation distance threshold `min_fdist`. Increasing `min_fdist` monotonically reduces the number of detected formation segments (Figure 10a), while the remaining change-points remain temporally stable (Figure 10b). This indicates that `min_fdist` primarily acts as a pruning mechanism that filters minor structural variations without altering the main segmentation.

Finally, varying the minimum period duration `min_pdur` does not affect either the number or the locations of detected change-points in this match, suggesting that the identified formation changes are temporally well separated and not driven by short-lived fluctuations.

4.2 Extensions to SoccerCPD

To enhance the interpretability of the tactical segments identified by SoccerCPD, we introduced two novel analytical layers: a contextual separation of formations based on possession and a quantifying metric for role fluidity.

4.2.1 Possession Context: Attacking vs. Defending Shapes

A limitation of the standard FormCPD output is that it produces a single "average" formation for a detected time segment. However, modern soccer teams adopt vastly different shapes depending on possession status. We extended the pipeline to filter frames based on the possession context (Attack vs. Defense, based on a centroid threshold since possession event data is unavailable for GPS tracking) before computing the formation centroids.

- **Attacking Formation:** Computed using only frames where the team is in possession.
- **Defensive Formation:** Computed using frames where the opponent is in possession.

The results, visualized in Figure 11 (Appendix D) for Match ID 1925299 (A-League, SkillCorner) and Figure 12 (FCBarcelona, StatsBomb), reveal significant structural differences that are lost in a global average. For both matches, the attacking shape is wider and higher up the pitch, whereas the defensive shape compresses, with wingers dropping deeper to form a compact block. This granular analysis confirms that a single "stable" phase detected by SoccerCPD actually comprises two distinct, alternating tactical configurations. The StatsBomb FCBarcelona match illustrates this particularly well, with the team shifting from a high-pressing 4-3-3 when attacking to a more conservative 4-4-2 block when defending. It must be noted, however, that the sparsity of event-stream data limits the precision of these formation estimates compared to high-frequency tracking data. This is why we see a player such as Pjanic, who typically plays as a central midfielder, being detected in a very deep defensive position in both the attacking and defensive formations of Phase 1. The events involving him mostly occur when the team is defending, leading to a biased estimation of his average position. That is not the case in phase 2, where he is detected in a more reasonable midfield position.

4.2.2 Player Stationarity Metric

While the original SoccerCPD model assigns a Gaussian mean (μ_k) and covariance (Σ_k) to each role, it does not explicitly quantify how strictly a player adheres to that role. We defined a Player Stationarity metric, calculated as the standard deviation of the Euclidean distance between a player's actual position and their assigned role's center (μ_k) over a formation phase. A lower value indicates a "fixed" positional role (e.g., a center-back holding the line), while a higher value indicates a "fluid" or "roaming" role. Applying this to the sampled StatsBomb FC Barcelona match, we observed distinct behavioral patterns. As shown in Figure 14 in Appendix D, midfield roles exhibited higher stationarity (lower deviation) compared to defensive fullbacks or attacking roles. For instance, during Phase 1, the average spatial deviation was approximately 9.8m, but specific attacking and even defensive roles showed deviations exceeding 12m, quantifying the "free-roaming" nature of Barcelona players compared to their midfielders, who distribute the ball and keep possession. These results can also be compared to phase 2 in Figure 15, where the average spatial deviation increased, as players were much more fluid in both attack and defense.

We also validated this metric on the A-League tracking data (Match ID 1925299), as illustrated

in Figure 13. The metric successfully captures the variance in player movement within a stable tactical phase, providing coaches with a concrete measure of positional discipline.

5 Conclusion

This report presented a comprehensive reproduction and extension of the SoccerCPD framework for detecting tactical formation changes in soccer using spatiotemporal data. We successfully implemented both stages of the pipeline, FormCPD and RoleCPD, verifying their effectiveness on synthetic datasets and real-world matches. Our contributions included the introduction of a player stationarity metric to quantify role fluidity, as well as the refinement of formation analysis by separating frames based on possession context (attack vs. defense). These extensions provided deeper insights into team tactics and individual player behaviors. We finally applied the adapted framework to event-stream data from the StatsBomb repository, demonstrating its versatility across different data types. Overall, our work validates the SoccerCPD approach while enhancing its interpretability and applicability in football analytics.

References

- [1] Alina Bialkowski, Patrick Lucey, Peter Carr, Yisong Yue, Sridha Sridharan, and Iain Matthews. Large-scale analysis of soccer matches using spatiotemporal tracking data. In *Proceedings of the IEEE International Conference on Data Mining (ICDM)*, pages 725–730. IEEE, 2014.
- [2] Hyunsung Kim, Bit Kim, Dongwook Chung, Jinsung Yoon, and Sang-Ki Ko. Soccercpd: Formation and role change-point detection in soccer matches using spatiotemporal tracking data. In *The 28th ACM SIGKDD Conference on Knowledge Discovery and Data Mining*, pages 3146–3156. ACM, 2022.
- [3] Jingru Zhang and Hao Chen. Graph-based two-sample tests for data with repeated observations, 2019.

A Appendix: Visual Examples for FormCPD

This appendix gathers all visual material related to the FormCPD pipeline (Role assignment, Delaunay encoding, and adjacency representations) referenced in Section 2.1.

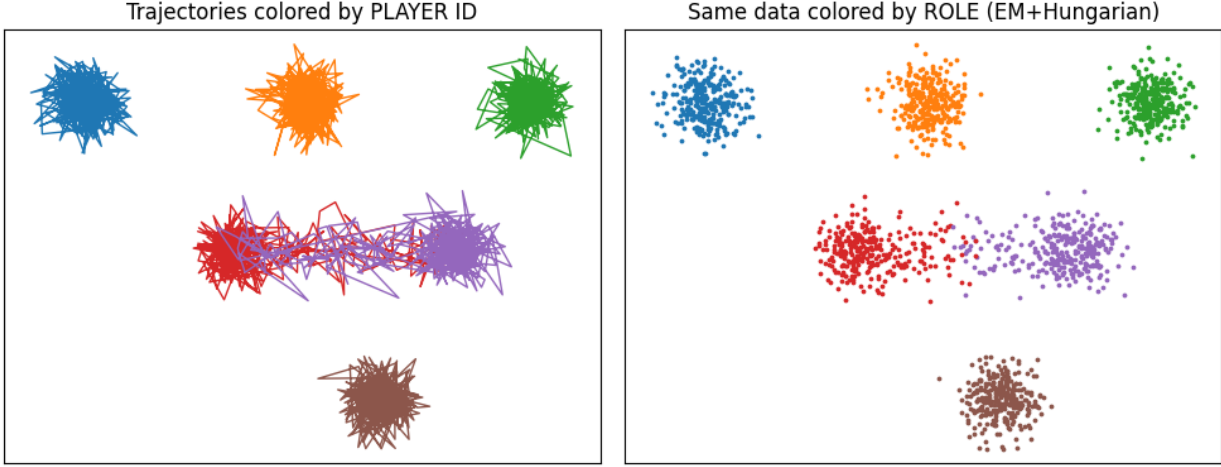


Figure 1: Player versus role-based coloring of trajectories during a simulated position swap.

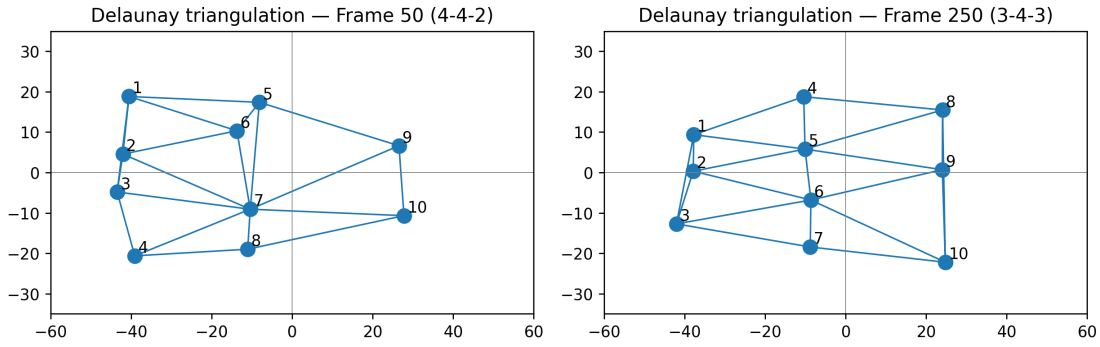
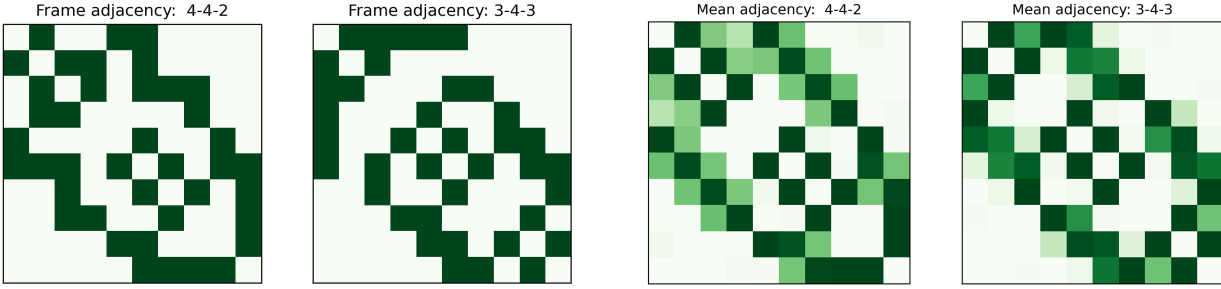


Figure 2: Delaunay triangulations of role locations at two frames before and after a synthetic formation change ($4-4-2 \rightarrow 3-4-3$).



(a) Single-frame binary adjacency matrices before and after the simulated formation change ($4-4-2 \rightarrow 3-4-3$) (Green = 1).

(b) Mean role-adjacency matrices averaged over each formation period (Green = 1).

Figure 3: Delaunay-based adjacency representation on a synthetic formation change.

B Appendix: Visual Examples for RoleCPD

This appendix gathers all visual material related to the RoleCPD pipeline (Hamming distance, Change Point Detection, and Segmentation) referenced in Section 2.2.

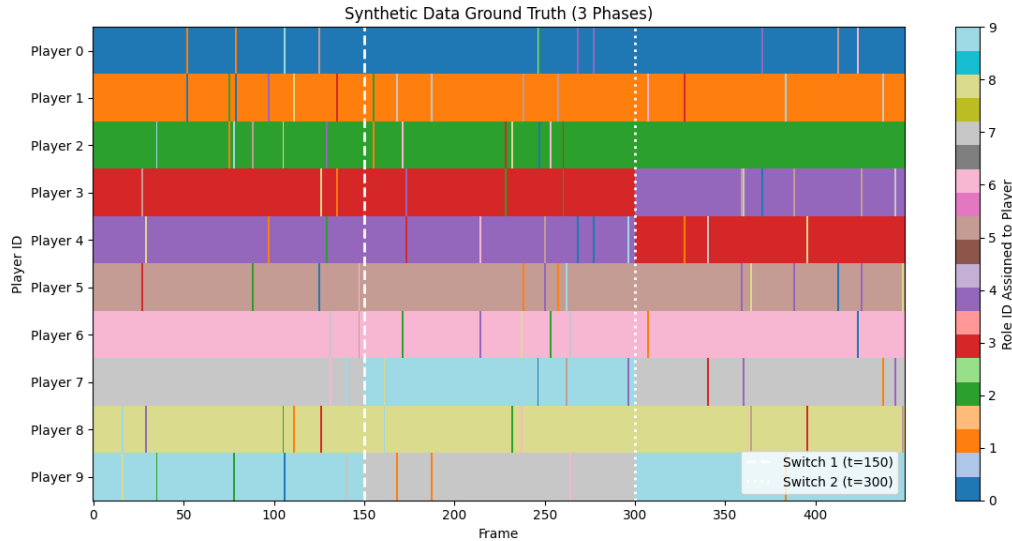


Figure 4: Ground truth role assignments over time with two tactical switches at frames 150 and 300.

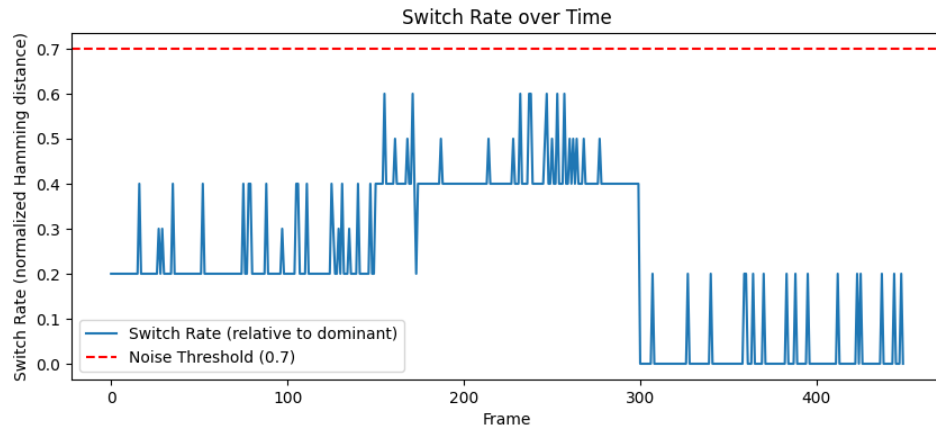


Figure 5: Hamming distance-based switch rate time series used for change point detection.

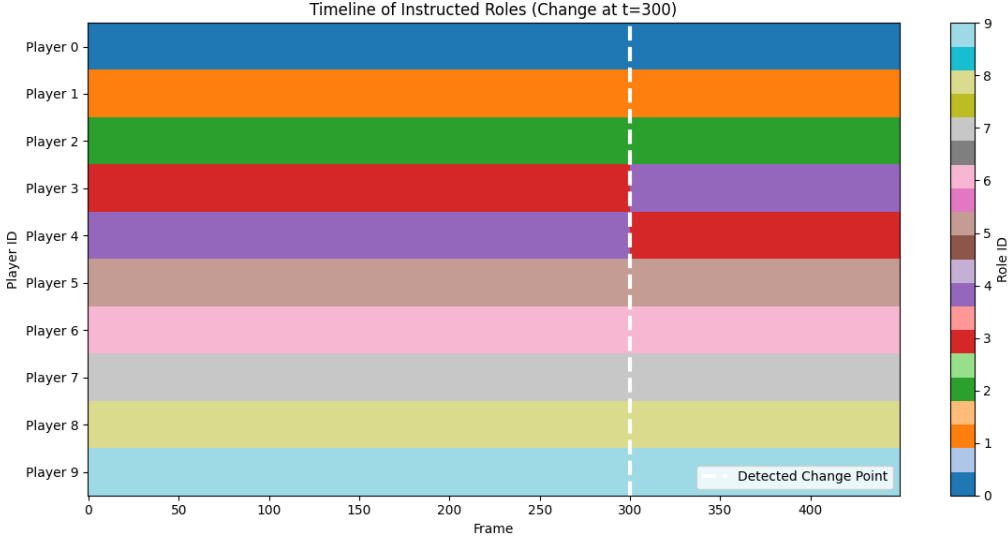


Figure 6: Visualization of one detected tactical phase with dominant role assignments. This shows the need for recursive segmentation to capture multiple phases.

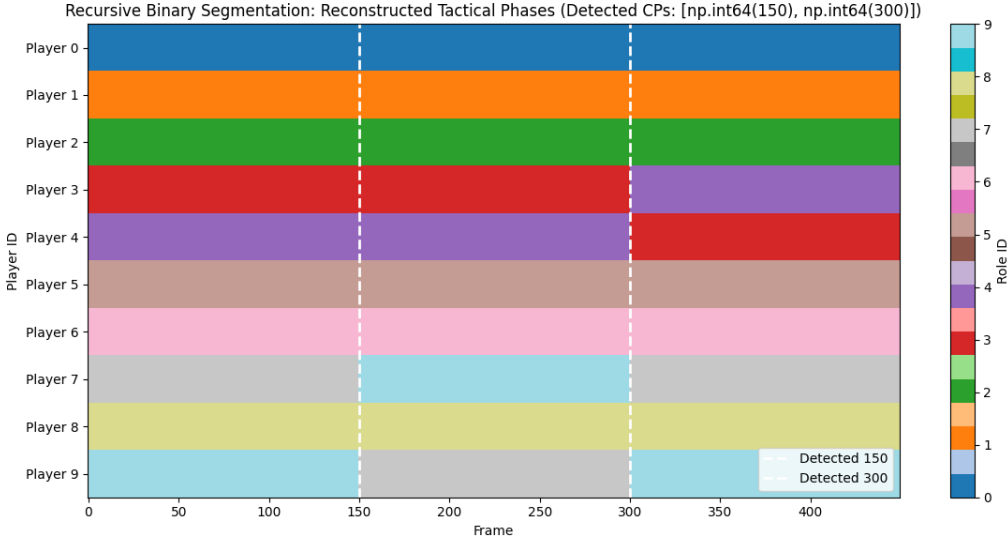


Figure 7: Visualization of all detected tactical phases after recursive binary segmentation, showing accurate recovery of the ground truth phases.

C Appendix: Visual Results for Data Analysis

This appendix gathers all visual material related to the data analysis referenced in Section 3.

Spatial Density and Signal Structure Comparison

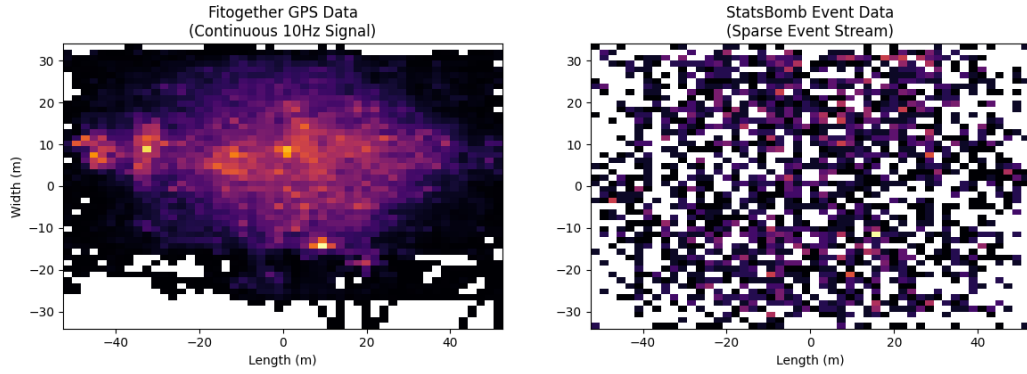


Figure 8: Spatial density comparison between continuous Fitogther GPS tracking data and StatsBomb event-based data (right). The GPS data shows continuous coverage of player positions, while the event data is sparse and concentrated around ball actions.

D Appendix: Visual Results for Experiments

This appendix gathers all visual material related to the experiments referenced in Section 4.

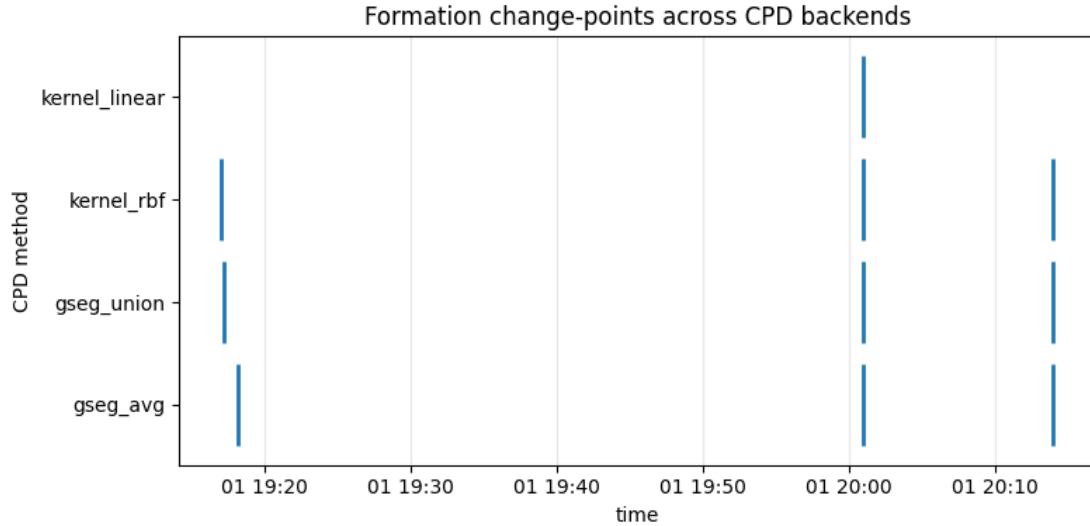


Figure 9: Formation change-points detected by different CPD backends on a common timeline.

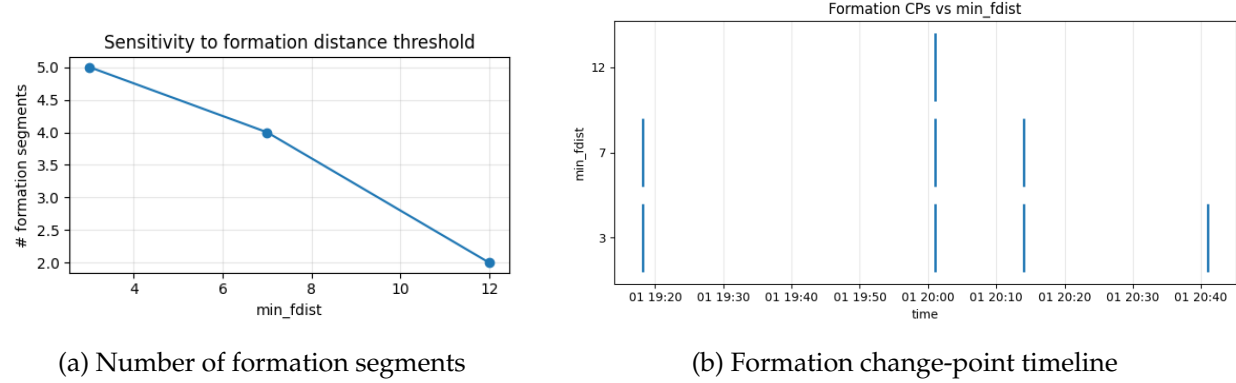


Figure 10: Sensitivity of formation change-point detection to the formation distance threshold min_fdist . Increasing the threshold reduces the number of detected segments while preserving the temporal locations of the most salient change-points.

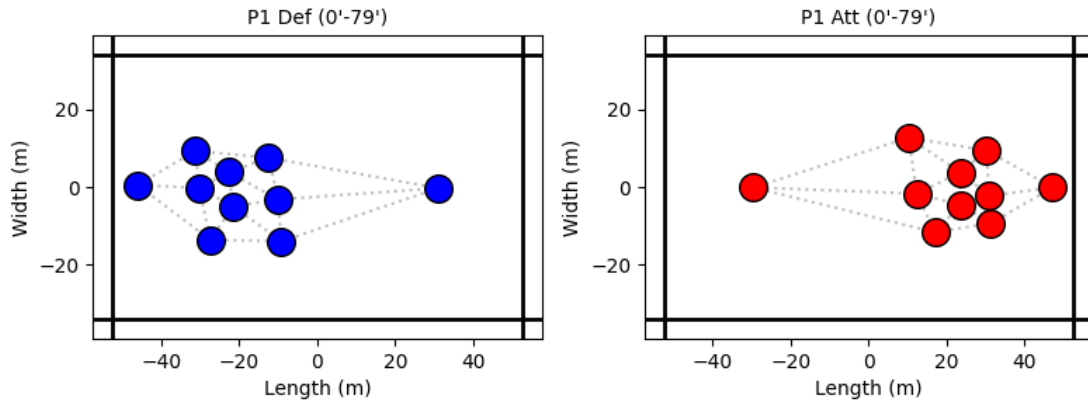


Figure 11: Detected formations for match "1925299" (A-League, SkillCorner) separated by phase of play: defending (left) vs. attacking (right). This highlights tactical adjustments based on possession context.

Detected Barcelona Formations by Phase (Attack vs Defense)

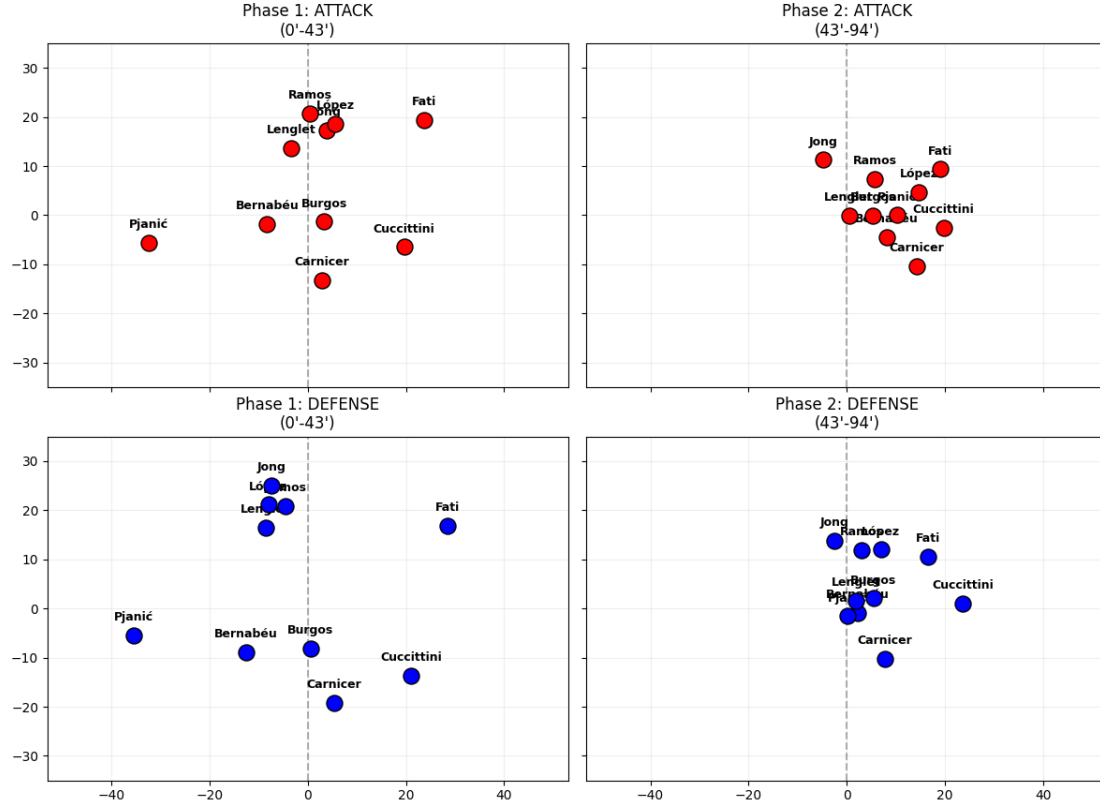


Figure 12: Detected formations for FC Barcelona using event-stream StatsBomb data separated by different tactical phases within the match. Each phase reflects a distinct formation strategy employed by the team.

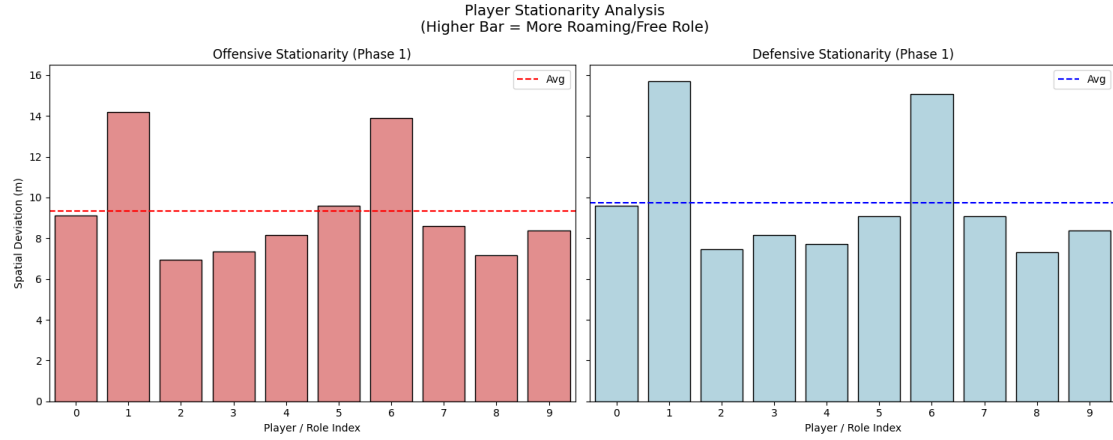


Figure 13: Player stationarity during Phase 1 of match "1925299" (A-League, SkillCorner), illustrating the consistency of player positions within the tactical phase.

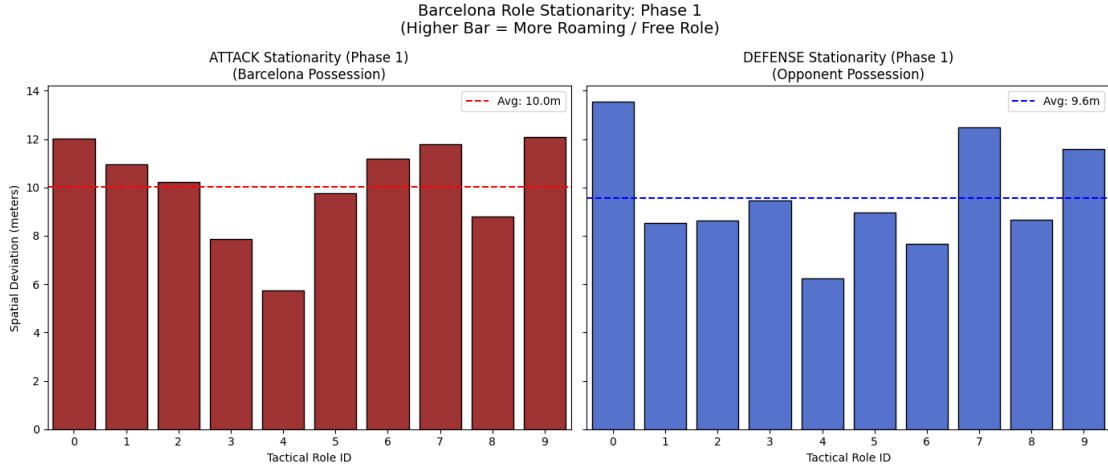


Figure 14: Player stationarity during Phase 1 of FC Barcelona match, illustrating the consistency of player positions within the tactical phase, even with event-stream data.

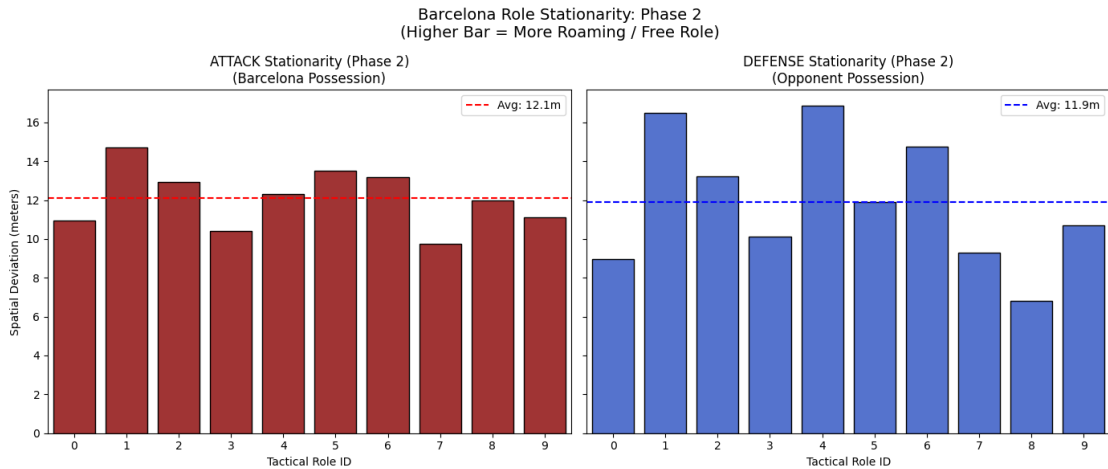


Figure 15: Player stationarity during Phase 2 of FC Barcelona match, illustrating the consistency of player positions within the tactical phase, even with event-stream data.